A Study of Galaxies with $z \leq 0.3$ in the ESO/SRC Atlas Field No. 411: Galaxy Distribution and Luminosity Functions

P. Schuecker
Astronomisches Institut
Westfälische Wilhelms-Universität
Münster, F.R. Germany

Abstract

The analysis of 6 300 galaxy redshifts obtained automatically from a single low-dispersion objective prism plate shows that the ESO/SRC Atlas field No. 411 is dominated by a galaxy supercluster at $z = 0.11 \pm 0.01$, $(330 \pm 30\, h^{-1} Mpc)$. The supercluster consists of at least five rich clusters, connected by bridges of galaxies, constituting a filament of length $> 20\, h^{-1}$Mpc. Luminosity functions are calculated for the high and low density regions. The fraction of bright galaxies is higher for the high density region.

1 Introduction

A number of authors have drawn attention to the observation and confirmation of super large-scale structures with dimensions of several tens to several hundreds of megaparsecs. Among them are Bahcall and Soneira (1983, 1984), Schmidt (1984), Batuski and Burns (1985) and Kopylov *et al.* (1987). In these investigations the assumption is made that rich clusters of galaxies trace superclusters, that their absence constitutes voids, and that the underlying distribution of galaxies follows the distribution of the clusters (Abell 1961). Because of the limited observing times at large telescopes most cluster distances are obtained from a few galaxy redshifts only. The interpretation of cluster catalogues (*e.g.* Schmidt 1986, Struble and Rood 1987a, b) with respect to super large-scale topology is thus complicated and not unique.

The present paper is the first of a series of communications about results from the Muenster Redshift Project (MRSP). The large-scale distribution of galaxies will be investigated in individual and in adjoining wide angle fields, with about 6 000 measured galaxy redshifts per field up to $z \leq 0.3$, and accuracies $dz = 0.008$ corresponding to $2\,400\,\mathrm{km\,s^{-1}}$. Special emphasis is given to the identification of clusters and superclusters, but also to the distribution of field galaxies. Horstmann (1988a, hereafter HH) in collaboration with the present author studies the distribution of galaxies of different morphological types. Luminosity functions for low and high density regions, *i.e.* field and cluster galaxies, are determined. All redshifts are obtained automatically from UK objective prism Schmidt plates (Schuecker 1988, hereafter PS).

2 General properties of the redshift sample

2.1 The observational data

16 800 galaxy spectra with a preset magnitude limit $m_J \leq 20^{\mathrm{m}}.5$ were segmented from the objective prism plate of field No. 411 (HH). 3 000 of the spectra overlap and were automatically rejected. From the remainder, 6 300 galaxy redshifts were determined with the methods described in PS. The galaxies have redshifts $0.0 \leq z \leq 0.3$ and magnitudes $16^{\mathrm{m}}.5 \leq m_J \leq 20^{\mathrm{m}}.5$.

The magnitudes were obtained by transforming m_J to m'_B using the mean colour index of the objects $B - V = 0.8$ and calibrating with the photometric sequence of Hawkins (1981). m'_B magnitudes are corrected for the K-effect using the analytic expression given by Shanks *et al.* (1984) for E and S0 galaxies:

$$m_B = m'_B - (4.14z - 0.44z^2) \tag{1}$$

The choice of correction factors is determined by the fact that early-type galaxies constitute about $\frac{2}{3}$ of the galaxies as found in the morphological studies of HH.

Corrections for biased redshift and magnitude measurements are necessary before luminosity functions (Sect. 4) can be derived.

2.2 Statistical corrections

In *Fig. 1a* differential galaxy number counts $N_d(m_B)$ in intervals of 0.1 magnitudes obtained from the direct plate and differential number counts for galaxies with mea-

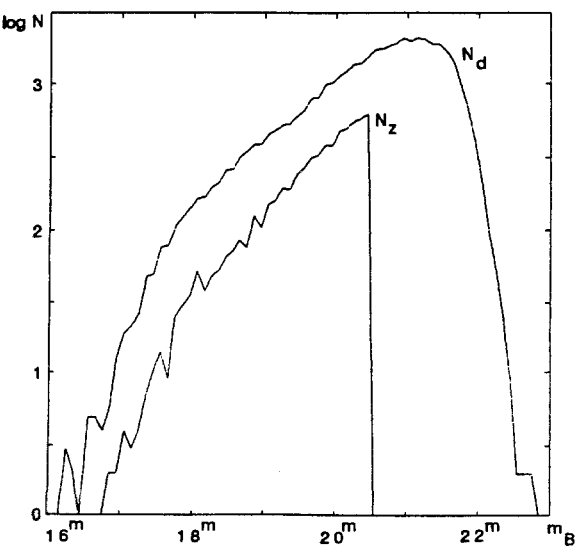

Fig. 1a. Differential galaxy number counts obtained from the direct plate $N_d(m_B)$ and for galaxies with measured redshifts $N_z(m_B)$ from the objective prism plate.

sured redshifts from the objective prism plate are shown. *Fig. 1b* gives the difference $s(m_B) = \log N_d(m_B) - \log N_z(m_B)$ for different magnitudes. The values of the $s(m_B)$-function measure the *incompleteness* of the redshift sample. The function is also sensitive to *biases* of the redshift sample relative to the sample from the direct plate.

Significant deviations from zero and from an unbiased flat distribution are found. Since higher values of $s(m_B)$ indicate a lower fraction of objects with measured redshifts it appears that increasingly more galaxies are missed going from faint to bright magnitudes down to about 17^{m}. This can be attributed to the fact that the galaxy images tend to be larger at bright magnitudes giving rise to a smeared out appearance and thus difficulties in measuring characteristic features. The small values of $s(m_B)$ for the brightest galaxies ($< 17^{\mathrm{m}}$) are an artefact. This is supported by the fact that the noise in this region is also high, due to the low number of objects (small volume covered in near space and scarcity of absolutely bright galaxies at larger distances).

Equation 2 is a formal description of the above mentioned selection effects:

$$s(m_B) = \begin{cases} 0.6500\, m_B - 10.2883, & m_B < 17\overset{\mathrm{m}}{.}0 \\ 0.1086\, m_B + 2.6079, & 17^{\mathrm{m}} \leq m_B \leq 20^{\mathrm{m}} \end{cases} \tag{2}$$

Eqn. 3 gives $N_z^c(m_B)$, the number of galaxies corrected for the selection effects, *i.e.* the expected unbiased number on the objective prism plate:

$$log N_z^c(m_B) = s(m_B) + \log N_z(m_B) \tag{3}$$

Because the correction factors are global they do not correct for differences in the redshift measurements of different galaxy types. The corrected sample is, of course, only complete and unbiased *relative* to the sample from the direct plate. Recent improvements of the techniques of redshift measurements show that our new data do not require a correction for bias. (Sect. 5 and Schuecker *et al.* 1988a).

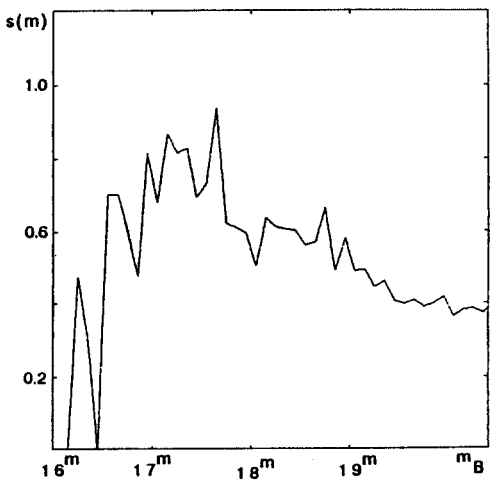

Fig. 1b. Logarithmic differences $s(m_B)$ for different magnitudes.

2.3 The $M(z)$-diagram

In *Fig. 1* of Ott (1988) absolute magnitudes M_B vs. redshifts z are plotted. The absolute magnitudes were calculated using the luminosity distance given by Mattig (1958), with the parameters $H_0 = 100$ km s^{-1} Mpc^{-1}, $q_0 = 0.5$ and $\Lambda = 0$:

$$M_B = m_B + 5\log H_0 - 25 - 5\log\left\{\frac{c}{q_0^2}[q_0 z + (q_0 - 1)(\sqrt{1 + 2q_0 z} - 1)]\right\} \quad (4)$$

In the $M_B(z)$ diagram the cutoff line is fixed by the limiting magnitude $m_B = 20^{\mathrm{m}}.5$. The lack of apparently bright galaxies at low redshifts ($z < 0.1$) is explained in Sect. 2.2.

3 Morphological properties of the redshift sample

3.1 The large-scale distribution of galaxies

Results concerning the two-dimensional distribution of galaxies for field No. 411 are given in Dodd and MacGillivray (1986) and in Horstmann (1988 a, b). Information about the individual clusters, *i.e.* distribution of galaxies in two and three dimensions, cluster luminosity functions etc., can be found in Schuecker *et al.* (1988b). *Fig. 2* shows the isopleths of galaxies in this field as presented by HH. The field is divided into five sections, a) to d) at different declinations and fixed right ascensions, and e) over a narrow right ascension strip covering all declinations included in a) to d).

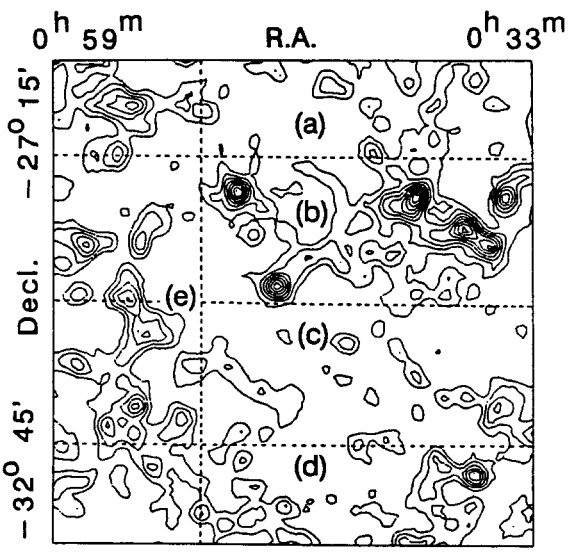

Fig. 2. The distribution of galaxies in field No. 411. For each section a) to e) corresponding wedge diagrams are shown in Fig. 3.

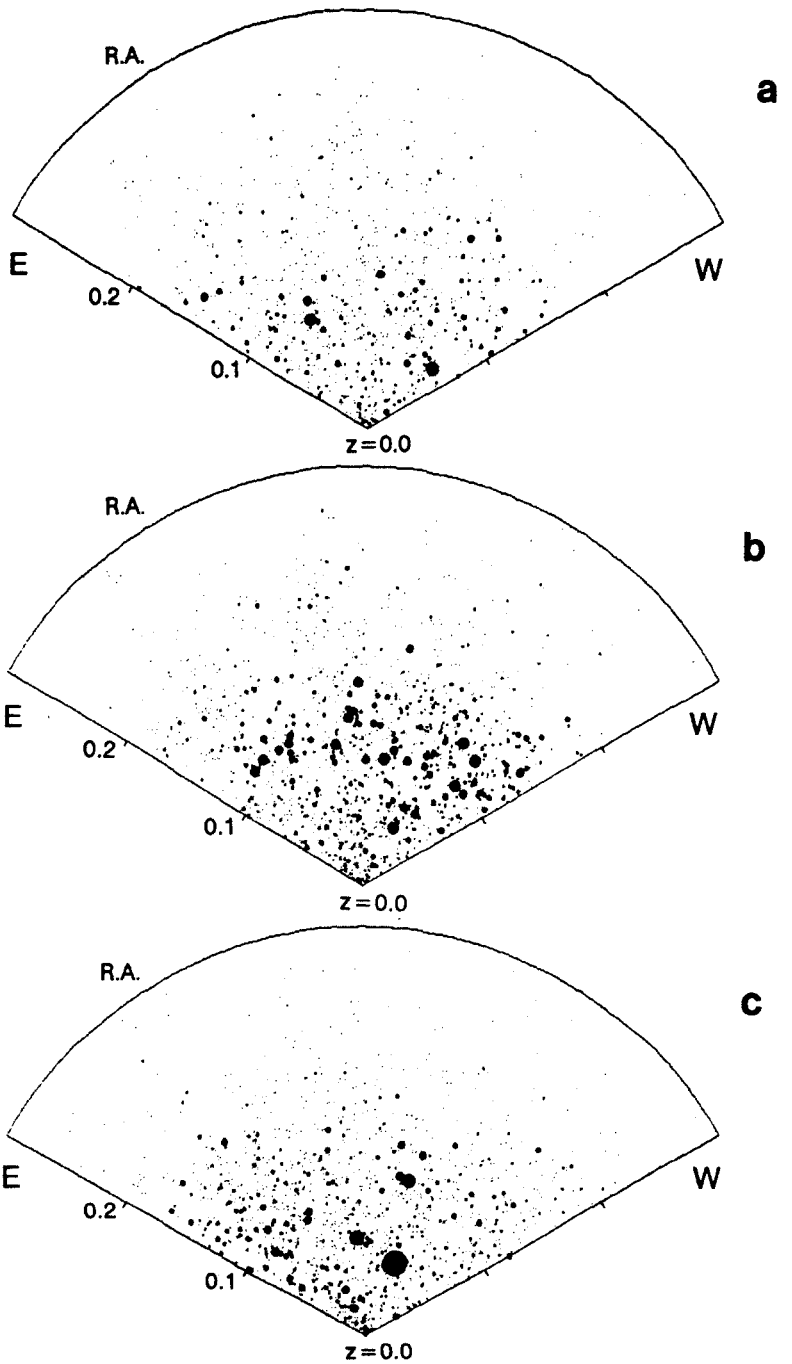

Fig. 3. Wedge diagrams of the five areas given in Fig. 2.
Fig. 3a: Section a) $0^h33^m \leq$ R.A. $\leq 0^h59^m$, $-28°21' \leq$ Decl. $\leq -27°15'$
Section b) $0^h33^m \leq$ R.A. $\leq 0^h59^m$, $-30°00' \leq$ Decl. $\leq -28°21'$
Section c) $0^h33^m \leq$ R.A. $\leq 0^h59^m$, $-31°39' \leq$ Decl. $\leq -30°00'$

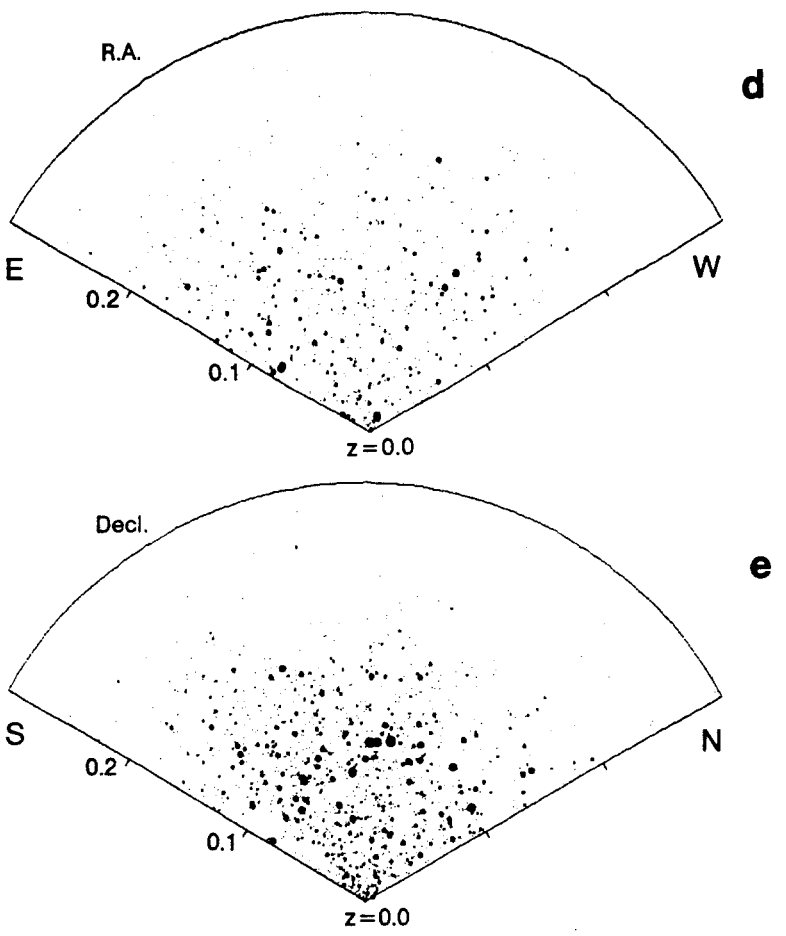

Fig. 3. cont.
Fig. 3b: Section d) $0^h33^m \leq$ R.A. $\leq 0^h59^m$, $-32°45' \leq$ Decl. $\leq -31°39'$
Section e) $0^h51^m \leq$ R.A. $\leq 0^h59^m$, $-32°45' \leq$ Decl. $\leq -27°15'$

Wedge diagrams of the five different areas are given in *Fig. 3.* The sizes of the symbols are proportional to the apparent brightness of the galaxies. *Fig. 3b* and e correspond to cluster-rich regions on the direct plate. The diagrams show that most of the luminous galaxies are concentrated in clusters near redshifts $z = 0.11$. Bright galaxies are also located at $z = 0.07$ (R.A. $= 0^h46^m$, Decl. $= -29°$) and $z = 0.12$ (R.A. $= 0^h55^m$, Decl. $= -30°$). In the other wedge diagrams no significant concentrations are found.

3.2 The redshift histograms

One hundred redshift histograms covering the whole field are presented in *Fig. 4.* Each histogram is calculated for an area of $33' \times 33'$. The redshift range is $0.0 \leq z \leq 0.3$. The galaxies are counted in bins $dz = 0.01$ leading to numbers of galaxies < 15 per bin. The average number per histogram is about 60.

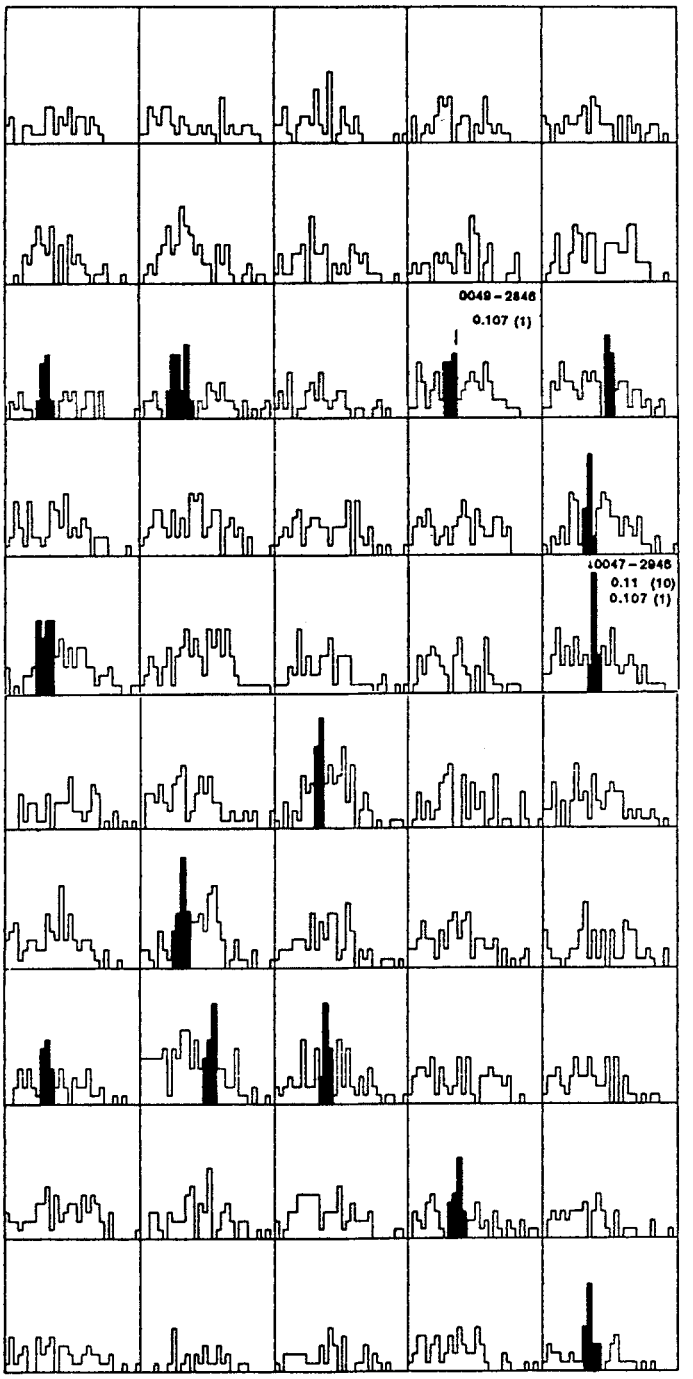

Fig. 4. Redshift histograms for field No. 411.
Fig. 4a: Section: $0^h46^m \leq$ R.A. $\leq 0^h59^m$, $-32°45' \leq$ Decl. $\leq -27°15'$

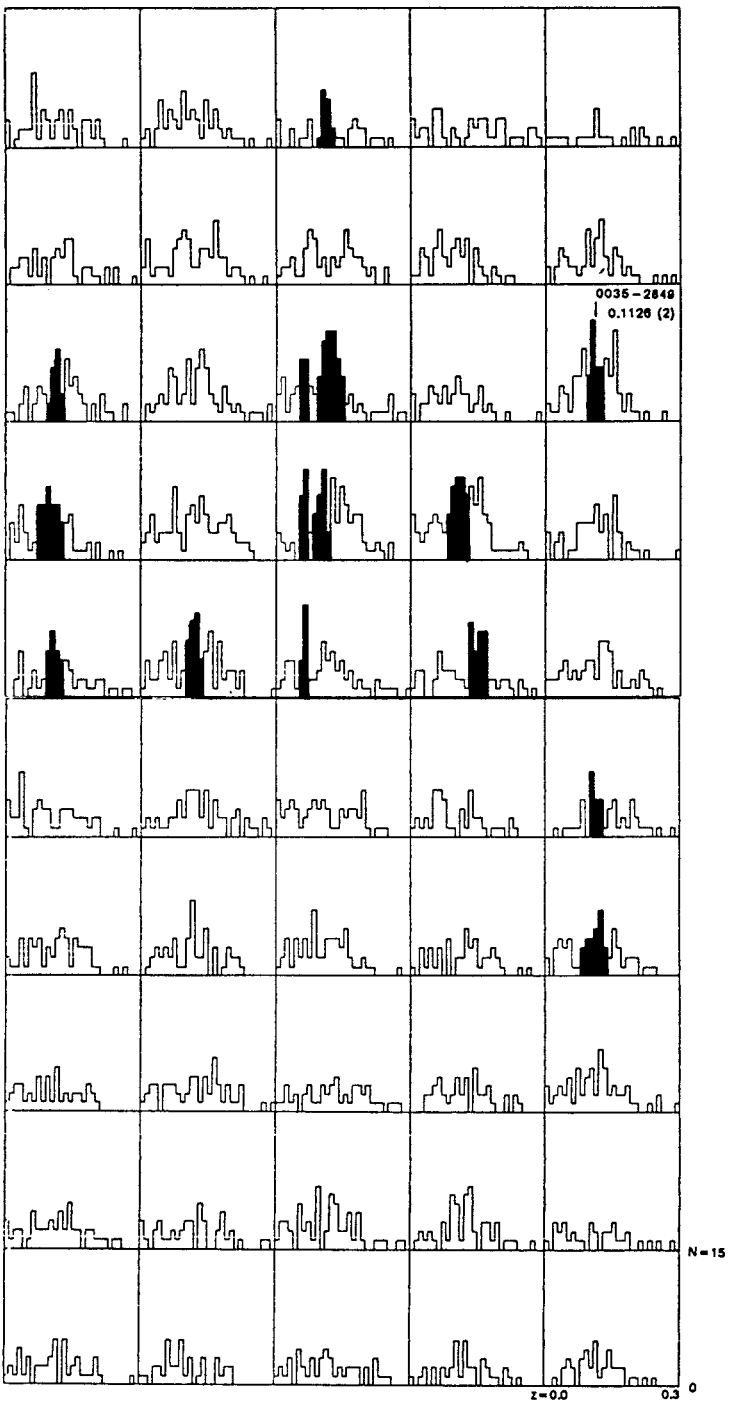

Fig. 4. cont.
Fig. 4b: Section: $0^h33^m \leq$ R.A. $\leq 0^h46^m$, $-32°45' \leq$ Decl. $\leq -27°15'$

As expected, the number of galaxies is larger in histograms from areas in the direction of the clusters than in the others. In these histograms the most significant columns are shaded. Most of them lie at redshifts $0.10 \leq z \leq 0.12$, again illustrating that the prominent clusters found on the direct plate are concentrated in this redshift range.

3.3 Comparison with previous measurements

Three of the five clusters have published redshifts obtained with slit spectra and objective prism spectra measured interactively. Table 1 lists the clusters, number of redshifts previously obtained, corresponding z-values, authors, number of galaxy redshifts measured in the MRSP and z-values obtained in the MRSP.

Table 1: Comparison of cluster redshifts

Cluster	N_{lit}	z	Authors	N_{MRSP}	z_{MRSP}
0035-2849	2	0.1126	1	20	0.105
0047-2946	1 (10*)	0.107 (0.11*)	2 (3*)	20	0.115
0049-2846	1	0.107	2	11	0.100

* interactive measurements from objective prism spectra

(1) West and Frandsen (1981)
(2) Ellis and Allen (1983)
(3) MacGillivray and Dodd (1979)

The external error of the MRSP cluster redshifts relative to those from other authors are not larger than the mean internal error of 0.008.

3.4 Clustering on large scales

The redshifts from Table 1 again support the existence of a concentration of the clusters at redshift $z = 0.11$. The question arises whether the clusters are part of a supercluster. If so, one expects to find connections between the clusters.

An interesting region in this context is at $0^{\mathrm{h}}47^{\mathrm{m}} \leq$ R.A. $\leq 0^{\mathrm{h}}49^{\mathrm{m}}$ and $-29°50' \leq$ Decl. $\leq -28°30'$ (*Fig. 4*). Of six histograms, four show prominent peaks at $z = 0.11$ or $z = 0.15$. Two of the histograms include the clusters 0047-2946 and 0049-2846, respectively. One 'non-cluster' histogram has a prominent peak at $z = 0.11$. On the direct plate a filament is seen connecting the centers of the two rich clusters. This suggests the existence of a bridge of galaxies about $6\,h^{-1}$Mpc long. The other non-cluster histogram has a peak at $z = 0.15$. This shows that the feature in spite of its close proximity to the 0.11-structure in projection is not a member of it.

Connections between the cluster pair 0047-2946, 0049-2846 in the eastern part and the cluster 0035-2849 in the western part of the 0.11-structure are apparent in the histograms for $0^{\mathrm{h}}35^{\mathrm{m}} \leq$ R.A. $\leq 0^{\mathrm{h}}46^{\mathrm{m}}$, $-28°15' \leq$ Decl. $\leq -30°00'$. Therefore,

the galaxies at $0.11\,c$ form a supercluster. The minimum size of the supercluster is $20\,h^{-1}$ Mpc in the direction of R.A. and $6\,h^{-1}$Mpc in the direction of Decl.

Measurements in neighbouring fields suggest a much larger size of the total supercluster ($> 40\,h^{-1}$ Mpc) in which the 0.11-structure constitutes the dominant region of very high density (see *Fig. 6* of HH).

The histograms for $0^h36^m \leq$ R.A. $\leq 0^h43^m$, $-30°15' \leq$ Decl. $\leq -28°15'$ have significant maxima at $z = 0.07$. The structure is also marked by some bright galaxies in the wedge diagrams (*Fig. 3*). This foreground cluster seems to be elongated with a major axis lying nearly perpendicular to the 0.11-structure. The smaller distance and the orientation of the cluster implies non-membership in the 0.11-structure.

4 Physical properties of the redshift sample

4.1 Parametric representation of luminosity functions

In order to give a physical description of the MRSP redshift sample luminosity functions (LF) were calculated.

Luminosity functions should be measured in equal redshift intervals Δz at different redshifts z. This guarantees good coverage of both the faint and bright ends of the LF. The number of galaxies at redshifts $z \pm \Delta z$ with magnitudes between M_B and $M_B + \Delta M_B$ is according to Weinberg (1972):

$$N(z \pm \Delta z, M_B)\,\Delta M_B = \left(\frac{c}{H_0}\right)^3 \frac{1}{q_0^4} \frac{[q_0 z + (q_0 - 1)(\sqrt{1 + 2q_0 z} - 1)]^2}{(1+z)^6 \sqrt{1 + 2q_0 z}}\, n(z, M_B)\, 2\Delta z\, \Delta\theta\, \Delta M_B\,, \quad (5)$$

$n(z, M_B)\,\Delta M_B$ is the number of galaxies per unit volume at redshift z with magnitudes between M and $M + \Delta M$.

If there is neither creation nor destruction and evolution of galaxies in the redshift range considered, the galaxy densities at redshifts z are related to the galaxy densities at $z = 0$ by

$$n(z, M_B) = (1+z)^3\, n(0, M_B)\,. \quad (6)$$

$n(0, M_B)$ is the general LF, *e.g.* the number of galaxies per proper unit volume.

According to the Schechter formalism (Schechter 1976) the LF is characterized by the parameters M_B^* (bright end magnitude), α (faint end slope) and n^* (normalization factor for galaxy densities). Whereas Schechter's analytic expression of the LF was originally formulated for luminosities, we use the magnitude dependent form:

$$\begin{aligned}\log[n(0, M_B)\,\Delta M_B] &= \log[0.4 \ln 10] + \log(n^*) - 0.4\,(\alpha + 1)\,(M_B - M_B^*) \\ &\quad - \log(e)\,\mathrm{dex}[-0.4\,(M_B - M_B^*)] + \log(\Delta M_B) \quad (7)\end{aligned}$$

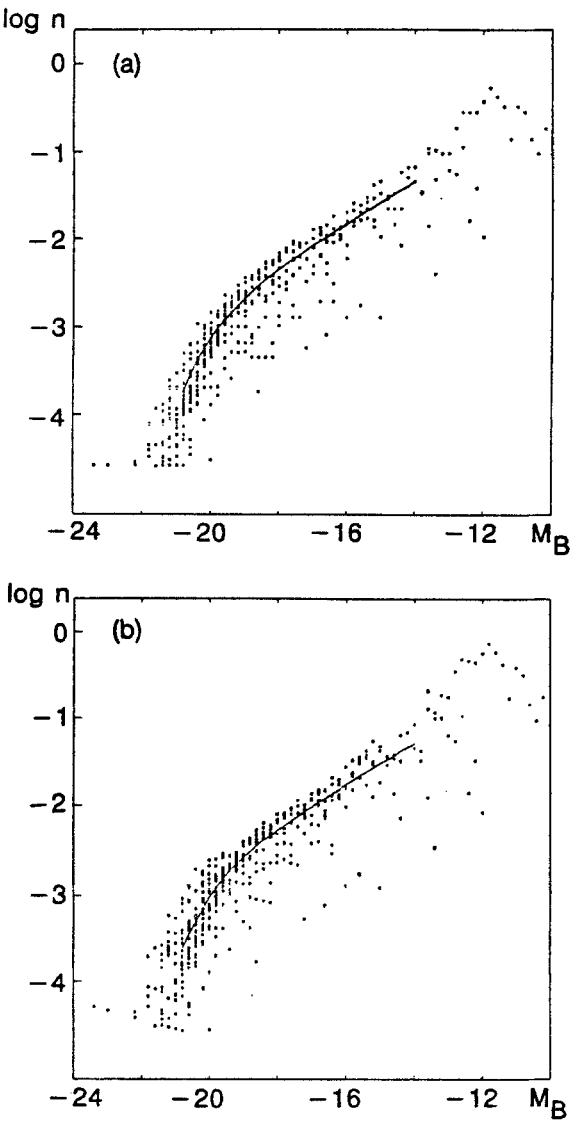

Fig. 5. Luminosity function of samples A (a) and B (b) with superimposed Schechter functions.

4.2 Luminosity functions of MRSP samples

In order to find possible differences between the LFs of the general field (low density) and the cluster regions (high density) five subsamples of the MRSP data were investigated:

Sample A: all galaxies with measured redshifts $0.0 < z \leq 0.3$
Sample B: sample A corrected for incompleteness and bias (Sect. 2.2)
Sample C: sample B for low density regions with $0.00 \leq z \leq 0.20$

Sample D: sample B for high density regions with $0.09 \leq z \leq 0.13$
Sample E: sample B for low density regions with $0.09 \leq z \leq 0.13$.

$n(0, M_B)$ is determined for the redshift intervals $2\Delta z = 0.01$ and the absolute magnitude intervals $\Delta M_B = 0.2$.

The comparison of samples A and B is used to show the influence of selection effects (Sect. 2.2) on the shape of the LF. Sample C is compared with the field LFs presented by Felten (1977). Samples D and E illustrate the differences between the shapes of the LFs for high and low density regions.

Figure 5 presents the LFs of samples A and B in the magnitude range $M_B = [-24, -10]$. The correction factors were computed separately for each $[z, z \pm \Delta z]$ and $[M_B, M_B + \Delta M_B]$ interval using Eqns. 1 through 4. Superimposed on *Fig. 5a* and *b* are the Schechter functions fitted to the data. The best-fit parameters and their formal errors are:

Sample A (uncorrected):
$M_B^* = -20\overset{\text{m}}{.}2 \pm 0.2, \quad \alpha = -1.58 \pm 0.07, \quad n^* = (3.7 \pm 0.5)10^{-3}$
Sample B (corrected):
$M_B^* = -20\overset{\text{m}}{.}2 \pm 0.2, \quad \alpha = -1.56 \pm 0.05, \quad n^* = (4.7 \pm 0.7)10^{-3}$

The logarithmic mean scatter of ± 0.2, corresponds to ratios of the $N(z \pm \Delta z, M_B)\,\Delta M_B$ of ± 1.6. The variances are caused by the clusters of galaxies found in the field and by the errors of the redshift and magnitude measurements. Measuring points with large deviations towards smaller n are systematically biased by the incompleteness of the sample; points with values $N(z \pm \Delta z, M_B)\,\Delta M_B < 5$ are not used for the fits with the Schechter function.

No significant differences between the LFs of the uncorrected and the corrected redshift samples are found. The use of the corrected galaxy number counts, however, increases n^*. The M_B^*-values are in general agreement with the values obtained *e.g.* by Sandage *et al.* (1985). The faint end slopes are smaller than the frequently quoted value $\alpha = -1.25$, but in good agreement with the data points in *Fig. 5*.

4.3 The field luminosity function

In *Fig. 6* the LF of sample C (field galaxies) is superimposed on the LFs assembled by Felten (1977). The mean number densities of field galaxies with equal absolute magnitudes in the present sample are determined using the same Hubble parameter $H_0 = 50\,\text{km}\,\text{s}^{-1}\,\text{Mpc}^{-1}$ and the same magnitude bin size $\Delta m_B = 1$ mag as Felten. Because field No. 411 is near the SGP no corrections for galactic absorption are applied. The MRSP data follow the general shape of the LFs with slightly lower densities in the range $-21^{\text{m}} \leq M_B \leq -18^{\text{m}}$. The densities at high luminosities are obtained from a few galaxies only. In order to get more reliable densities in this magnitude range, additional measurements on other plates are in preparation.

Table 2: Comparison of luminosity functions

	M_B^* (mag)	α	n^* (10^{-3})
High density region	-20.4 ± 0.4	-1.4 ± 0.1	14.4 ± 4.3
Low density region	-22.5 ± 0.4	-1.7 ± 0.1	1.0 ± 0.2

4.4 Comparison of luminosity functions in high and low density regions

The LFs of samples D and E, fitted with Schechter functions, are shown in *Fig. 7.* The best-fit parameters are given in *Table 2.*

The LFs and the best-fit parameters suggest that the fraction of bright (giant) galaxies is higher in clusters than in the general field. At present it is not clear whether this effect is caused by the properties of field and cluster galaxies, selection effects depending on morphology (*e.g.* the fraction of spiral galaxies is higher for the general field) and/or instrumental effects (*e.g.* variation of the sensitivity of the emulsion across the plate).

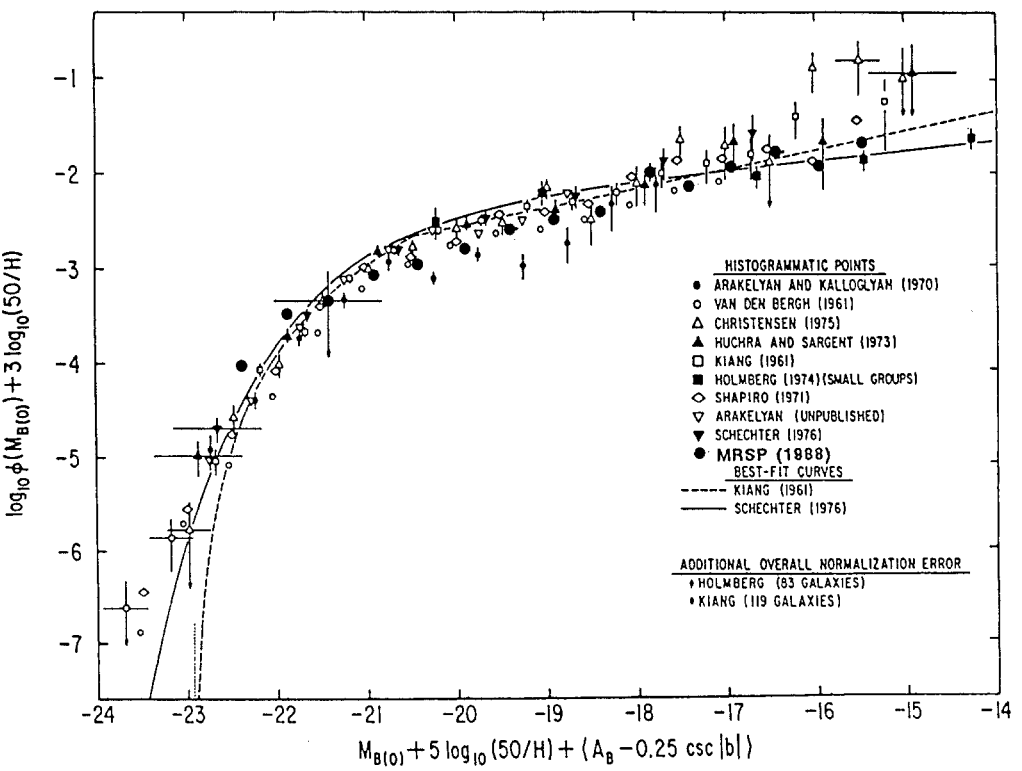

Fig. 6. The luminosity function of sample C superimposed on the luminosity functions assembled by Felten (1977).

5 Conclusions

A sample of 6 300 galaxies with redshifts $z \leq 0.3$ was analyzed. The results are:

- Five rich clusters are found at $z = 0.11$. For three of the clusters redshifts are available from slit spectra, supporting the present results.
- The rich clusters at $z = 0.11$ are connected and members of the **Sculptor supercluster** with a confirmed size of about $20\,h^{-1}$ Mpc and a possible extend $> 40\,h^{-1}$ Mpc. In the latter case the 0.11-structure constitutes a dominant (very high density) nucleus of the supercluster.
- The often used hypothesis that galaxies which are not members of rich clusters do follow the distribution of the clusters (Abell 1961, Einasto *et al.* 1980) is supported by the presence of extended bridges between the clusters.
- Possible clusters are found at $z = 0.07$ and $z = 0.15$, respectively.
- After correcting for the incompleteness of the redshift sample using corresponding galaxy number counts on the direct plate, luminosity functions were calculated. For the field galaxies the luminosity function is in general agreement with Felten (1977).
- Significant differences between the luminosity functions for high and low density regions are observed. It is not yet clear whether these differences are physically real.

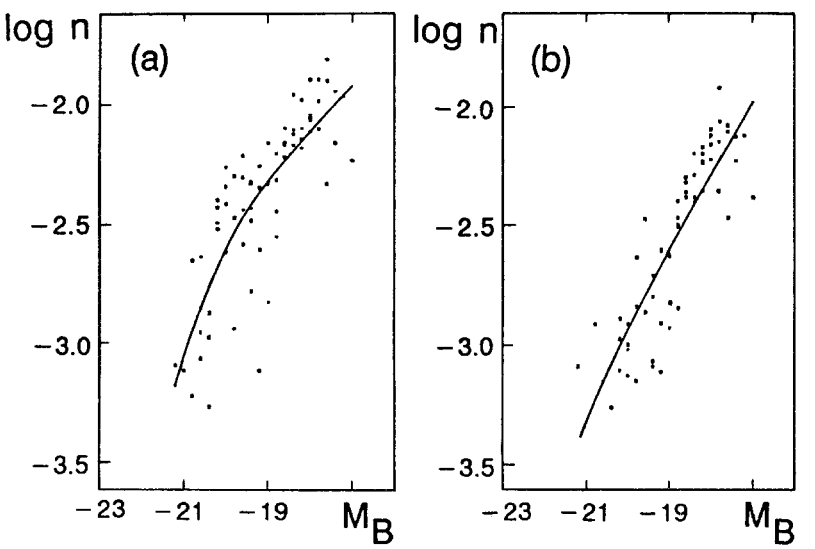

Fig. 7. Luminosity function of sample D (a) and E(b) with superimposed Schechter functions.

6 Prospects

Recent improvements of the redshift measurement methods have increased the completeness of the redshift sample, giving 7 200 galaxy redshifts with $m \leq 20^{\mathrm{m}}$ instead of 6 300 redshifts with $m_B \leq 20^{\mathrm{m}}.5$ for the sample discussed in this paper.

Redshifts were also obtained in fields adjacent to field No. 411. They yield 4 000 redshifts (No. 351), 4 300 redshifts (No. 474), 8 200 redshifts (No. 412). The large variations in the number of redshifts are mainly caused by differences in the quality of the objective prism plates. The redshift histograms of this enlarged sample of 23 700 galaxies support the existence of the 0.11 supercluster with possible extensions in field No. 412 and No. 474. Other concentrations of clusters of galaxies are found in field No. 351 suggesting the presence of another supercluster at $z = 0.14$.

Acknowledgements

This work is supported by the Deutsche Forschungsgemeinschaft. I thank H.-A. Ott for useful discussions about the luminosity functions.

References

Abell, G.O., 1961. *Astr. J.*, **66**, 607.
Bahcall, N.A., Soneira, R.M., 1983. *Astrophys. J.*, **270**, 20.
Bahcall, N.A., Soneira, R.M., 1984. *Astrophys. J.*, **277**, 27.
Batuski, D.J., Burns, J.O., 1985. *Astrophys. J.*, **299**, 5.
Dodd, R.J., MacGillivray, H.T., 1986. *Astr. J.*, **92**, 706. Einasto, J., Joeveer, M., Saar, E., 1980. *Mon. Not. R. astr. Soc.*, **193**, 353.
Ellis, R.S., Allen, D.A., 1983. *Mon. Not. R. astr. Soc.*, **203**, 685.
Felten, J.E., 1977. *Astr. J.*, **82**, 861.
Hawkins, M.R.S., 1981. *Mon. Not. R. astr. Soc.*, **194**, 1013.
Horstmann, H., 1988a. *These proceedings*, p. 111.
Horstmann, H., 1988b. In *IAU Workshop Astrophotography*, ed. Marx, S., Springer, Berlin, p. 186.
Hubble, E., Humason, M.L., 1931. *Astrophys. J.*, **74**, 43.
Kopylov, A.I., Kuznetsov, Yu., Fetisova, T.S., Shvartsman, V.F., 1987, *The Large-Scale Structure of the Universe*, Izd. Spets. Astrofiz. Obs., Stavropol', p. 39.
MacGillivray, H.T., Dodd, R.J., 1979. *Mon. Not. R. astr. Soc.*, **186**, 743.
Mattig, W., 1958. *Astr. Nachr.*, **284**, 109.
Ott, H.-A., 1988. *These proceedings*, p. 274.
Sandage, A., Bingelli, B., Tammann, G.A., 1985. *Astr. J.*, 90, 1759.
Schechter, P., 1976. *Astrophys. J.*, **203**, 297.
Schmidt, K.-H., 1984. *Clusters and Groups of Galaxies*, eds. Mardirossian, F., Giuricin, G., Mezzetti, M., Reidel, Dordrecht, p. 73.
Schmidt, K.-H., 1986. *Astr. Nachr.*, **307**, 69.
Schuecker, P., 1988. *These proceedings*, p. 142.
Schuecker, P., Ott., H.-A., Horstmann, H., Gericke, V., Seitter, W., 1988a. *3rd ESO-CERN Conf. on Cosmology*, Kluwer, Dordrecht, in press.
Schuecker, P., Horstmann, H., Seitter, W., 1988b. *IAU Symp. 130, The Structure of the Universe*, eds. Audouze, J., Szalay, A., Kluwer, Dordrecht, in press.

Shanks, T., Stevenson, P.R.F., Fong, R., MacGillivray, H.T., 1984. *Mon. Not. R. astr. Soc.*, **206**, 767.
Struble, M.F., Rood, H.J., 1987a, *Astr. J.*, **93**, 1035.
Struble, M.F., Rood, H.J., 1987b, *Astrophys. J. Suppl.*, **63**, 543.
Weinberg, S., 1972. *Gravitation and Cosmology*, Wiley, New York.
West, R.M., Frandsen, S., 1981. *Astr. Astrophys. Suppl.*, **44**, 329.